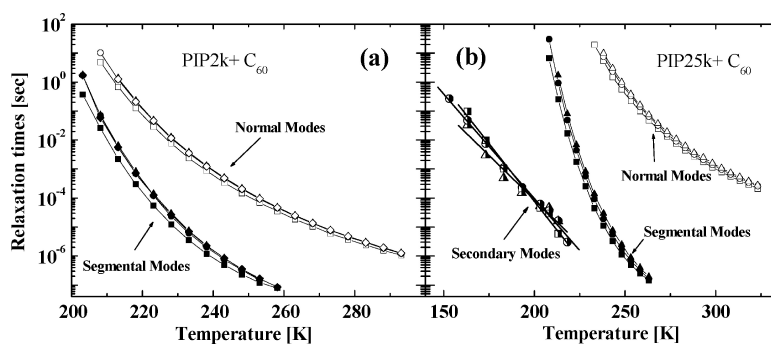


## Dielectric Spectroscopy Investigation of Relaxation in C<sub>60</sub>Polyisoprene Nanocomposites

Yifu Ding, Sebastian Pawlus, Alexei P. Sokolov, Jack F. Douglas, Alamgir Karim, and Christopher L. Soles

*Macromolecules*, 2009, 42 (8), 3201-3206 • DOI: 10.1021/ma8024333 • Publication Date (Web): 23 March 2009

Downloaded from <http://pubs.acs.org> on April 21, 2009



### More About This Article

Additional resources and features associated with this article are available within the HTML version:

- Supporting Information
- Access to high resolution figures
- Links to articles and content related to this article
- Copyright permission to reproduce figures and/or text from this article

[View the Full Text HTML](#)

# Dielectric Spectroscopy Investigation of Relaxation in C<sub>60</sub>–Polyisoprene Nanocomposites

Yifu Ding,<sup>\*,†</sup> Sebastian Pawlus,<sup>‡,§</sup> Alexei P. Sokolov,<sup>‡</sup> Jack F. Douglas,<sup>\*,||</sup> Alamgir Karim,<sup>||,⊥</sup> and Christopher L. Soles<sup>||</sup>

Department of Mechanical Engineering, University of Colorado at Boulder, Boulder, Colorado 80309-0427, Department of Polymer Science, University of Akron, Akron, Ohio 44325-3909, Institute of Physics, University of Silesia, 40-007 Katowice, Poland, Polymers Division, National Institute of Standards and Technology, Gaithersburg, Maryland 20899

Received October 30, 2008; Revised Manuscript Received January 15, 2009

**ABSTRACT:** We investigate the influence of adding C<sub>60</sub> nanoparticles on the dielectric relaxation spectra of both unentangled and entangled polyisoprene (PIP). Relaxation modes corresponding to both the segmental and chain relaxation were analyzed over a broad temperature and frequency range. Regardless of whether the chains were entangled or not, both relaxation processes slowed down with the addition of C<sub>60</sub>, reflecting an increase of the nanocomposite glass transition temperature. However, C<sub>60</sub> affects the segmental relaxation more strongly than the large-scale chain relaxation, both in terms of the relaxation time and strength, suggesting that the effect of the nanoparticles on the polymer dynamics is scale dependent. This effect is attributed to a difference in packing frustration at different length scales, a phenomenon also relevant to understanding the difference between the temperature dependence of the segmental and chain relaxation processes in neat polymer materials. Further evidence of this scale dependence is indicated by the observation that the secondary relaxation time of the high molecular mass PIP decreases with an addition of C<sub>60</sub>. These observations indicate that C<sub>60</sub> has an effect *opposite* to antiplasticizing additives that slow down the secondary relaxation (stiffening the material) in the glass state, while at the same time reducing the alpha relaxation time associated with cooperative segmental and chain motions. Recent incoherent neutron scattering measurements have indicated that C<sub>60</sub> can have a similar effect on polystyrene.

## Introduction

Nanoparticles, such as C<sub>60</sub>, have a great potential for a wide range of applications.<sup>1–14</sup> The large surface-to-volume ratio, electrical conductivity, and well-defined geometry and interactions of these model nanoparticles make them ideal additives for modifying the properties of polymers and as model nanocomposite systems for investigating the origin of these property changes from a fundamental perspective.

The properties of polymer fluids are dominated by the physics of glass formation and glass-forming liquids are intrinsically heterogeneous materials at a nanoscale. Much of the promise, as well as the complexity, of nanoparticle additives derive from their potential to alter the heterogeneous structure of polymeric glass-forming liquids. Once this aspect of the nanoparticles is realized, significant changes in the nature of glass formation can be expected to occur with some nanoparticle additives, and continuum-based filler models are of little help in understanding such property changes. Modifications of the properties of the polymer glass also imply corresponding changes of the viscoelastic properties of the polymer melt at much longer time scale through the monomer friction coefficient. There is thus a “trickle down” effect on the dynamics of the nanocomposite from atomic scales, then the scale of the chain statistical segment and even larger scales comparable to the chain radius of gyration or larger.

Recently, many experimental and simulation studies have been carried out to understand the influence of nanoparticles

such as C<sub>60</sub> on the glass formation, as well as the viscoelastic properties of the polymer nanocomposites.<sup>15–27</sup> De Pablo and co-workers showed that nanoparticles can modify the elastic constant fluctuations of the matrix at nanoscale dimensions, especially in the vicinity of the particle surfaces.<sup>17,18</sup> Inelastic neutron scattering measurements by Sanz et al. indicate that the addition of a small amount of C<sub>60</sub> (≈1% by mass) to polystyrene (PS) caused an increase in the Debye–Waller factor, reflecting an increase of the local compliance of the material, while at the same time an increase of  $T_g$  was observed.<sup>16</sup> In C<sub>60</sub>-polymethyl-methacrylate (PMMA) nanocomposites, both  $T_g$  and the “terminal” (chain relaxation time of an entangled polymer melt) relaxation time of the system were observed to increase with the C<sub>60</sub> addition, which was attributed to the increase of monomer friction coefficient.<sup>20</sup> In contrast, a significant reduction of the shear viscosity of the PS melt was reported upon the addition of C<sub>60</sub>.<sup>21</sup> Notably, the shear viscosity is roughly the product of the shear modulus and the stress relaxation time so it is unclear whether these reported trends are inconsistent. It is possible that nanoparticle additives can significantly decrease the stiffness (shear modulus) of the material, while simultaneously increasing the stress relaxation time.

The studies mentioned above collectively indicate that nanoparticles, such as C<sub>60</sub>, can cause a significant perturbation to the dynamics of polymeric matrix materials. However, these measurements involve different frequency and spatial scales and it is difficult to gain a complete picture of how atomic, segmental and chain scale relaxations are perturbed by nanoparticle additives. A full understanding of these changes is necessary if the *qualitative* nature of glass formation process is modified by nanoparticle additives, as discussed above.

Here we use broadband dielectric spectroscopy (BDS) to directly measure the influence of C<sub>60</sub> on the polymer relaxations corresponding to different length and time scales. BDS is one of the most efficient tools in studying molecular relaxations of

\* To whom correspondence should be sent. E-mail: (Y.D.) yifu.ding@colorado.edu; (J.F.D.) jack.douglas@nist.gov.

<sup>†</sup> Department of Mechanical Engineering, University of Colorado at Boulder.

<sup>‡</sup> Department of Polymer Science, University of Akron.

<sup>§</sup> Institute of Physics, University of Silesia.

<sup>||</sup> Polymers Division, National Institute of Standards and Technology.

<sup>⊥</sup> Present address: Department of Polymer Engineering, University of Akron, Akron, OH 44325-0301.

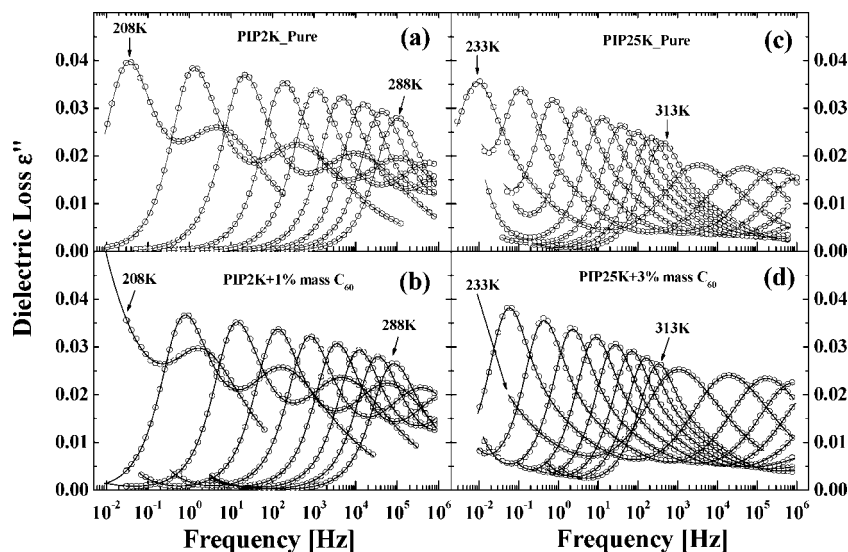


**Figure 1.** Representative dielectric loss spectra ( $\epsilon''$ ) at different temperatures of (a) PIP2k, (b) PIP2k mixed with 1% mass  $C_{60}$ , (c) PIP25k, and (d) PIP25k with 3% mass  $C_{60}$ . For the PIP2k system, (a and c), corresponding temperature increases from 208 to 288 K, with a step of 10 K. For the PIP25k system, corresponding temperature increases from 233 to 313 K with a step of 10 K. The symbols represent the measurement data, and the lines represent the fitting result using the Havriliak–Negami function.

polymers. It covers a broad frequency range, allowing measurement of different relaxation processes simultaneously, including secondary, the segmental relaxation associated with glass transition, and even entire chain relaxations processes under favorable circumstances.<sup>23,28–30</sup> The high resolution of the BDS permits analysis of the subtle changes in these relaxation modes associated with molecular motions on different length scales.

In this paper, we report the BDS measurements on the  $C_{60}$ –*cis*-polyisoprene (PIP) nanocomposites. *cis*-PIP is a so-called type A polymer (according to Stockmayer's definition<sup>31</sup>) that contains dipole moments both perpendicular and parallel to the backbone of the chain.<sup>28,29,32–39</sup> The accumulated dipole moment parallel to the backbone is equivalent to the root-mean-square end-to-end vector ( $\langle R^2 \rangle^{1/2}$ ) of the chain. The relaxations of perpendicular and parallel dipole moments give rise to the segmental and chain relaxation processes respectively. Our measurements reveal that all the relaxation modes are affected by  $C_{60}$ . However, the effects are strongly mode specific, indicating that even the *qualitative* nature of the changes in the polymer dynamics with the nanoparticle additive can be length and time scale dependent.

## Experimental Section

Two monodisperse PIP samples were purchased from Polymer Source,  $M_n = 2000$  g/mol with a polydispersity index (PDI) of 1.08, and  $M_n = 25\,000$  g/mol with a PDI of 1.04. They are termed PIP2k (unentangled since the entanglement molecular mass of PIP is about 5000 g/mol<sup>40</sup>) and PIP25k (entangled) throughout this paper for simplicity. The  $C_{60}$  sample was purchased from Sigma-Aldrich. All materials were used without further purification.

Due to the low  $T_g$  of PIP (200 to 210 K), it is difficult to prepare the  $C_{60}$ –PIP composites through the precipitation methods discussed in ref 7. Instead, a conventional solvent evaporation approach was used for preparing the  $C_{60}$ –PIP nanocomposites.<sup>15,20,41</sup> A dilute solution of  $C_{60}$  in toluene was prepared via sonication for 20 min, until a homogeneous, clear solution was obtained. PIP was then added to the solution to achieve the desired  $C_{60}$  concentration in the final composites. The covered solution was then put in a shaker for 2 h to ensure a homogeneous solution was obtained. The solutions were then placed under the flow of  $N_2$  to evaporate the majority of the toluene, before transferring to a vacuum oven for 48 h at room temperature to remove the residual solvent. Using this approach, a series of concentrations for  $C_{60}$ –PIP composites

were prepared: 0.1% mass, 0.5% mass, 1% mass, and 3% mass for PIP2k, and 0.5% mass and 3% mass for PIP25k. Except for a PIP2k sample having a relatively high fullerene concentration (3% mass  $C_{60}$ ), all samples were optically clear and no aggregates were visually apparent under an optical microscope.

Aggregates of fullerenes are expected at smaller scales, however. This general phenomenon is illustrated by Kropka et al. in measurements where PMMA is the matrix,<sup>20</sup> and clustering has also been observed for PS and other polymers.<sup>42,43</sup> In particular, transmission electron microscopy (TEM) measurements by Kropka indicate aggregates on the order of 10 to 20 nm for low  $C_{60}$  concentrations,  $\varphi \leq 1\%$  mass, so these clusters remain basically nanoparticles in this low concentration regime.<sup>20</sup> The clusters normally become macroscopic in dimensions for  $\varphi$  between 3% mass to 4% mass and large clusters of this kind have recently been imaged in  $C_{60}$ –PS nanocomposite films.<sup>44</sup> Our measurements for  $C_{60}$ –PIP nanocomposite span a concentration range where  $C_{60}$  should be reasonably well dispersed at low concentration and only nanoscale particles should exist.

Our dielectric measurements were performed using a Novocontrol Alpha Impedance Analyzer in the frequency range from 1 mHz to 3 MHz at different temperatures.<sup>45</sup>  $C_{60}$ –PIP liquid samples were placed into a parallel-plate capacitor with 20 mm diameter, and a pair of glass fibers with 40  $\mu\text{m}$  diameter was used as the spacers between the electrodes. The sample capacitor was mounted in the fixture and placed in the cryostat. Temperature stabilization was better than 0.1 K throughout the measurements. The temperature control was achieved through Novocontrol Quatro Cryosystem and data analysis was performed through Novocontrol WinFit program.

## Results and Discussion

Figure 1 presents the dielectric loss spectra ( $\epsilon''$ ) of both pure PIP control samples (parts a and c) and representative  $C_{60}$ –PIP composites samples (parts b and d) measured at different temperatures. All of the relaxation processes are well separated in these measurements, providing a good opportunity for analyzing their dependence on the  $C_{60}$  concentrations at different temperatures. The higher frequency relaxation process corresponds to the segmental mode, which is associated with the glass transition of the system. The lower frequency relaxation process is associated with the relaxation of the chain as a whole and is often designated the “normal mode” relaxation process.

Figure 2 shows the dielectric relaxation spectra at 183 K (below  $T_g$  of both pure PIP samples) for both  $C_{60}$ –PIP systems.

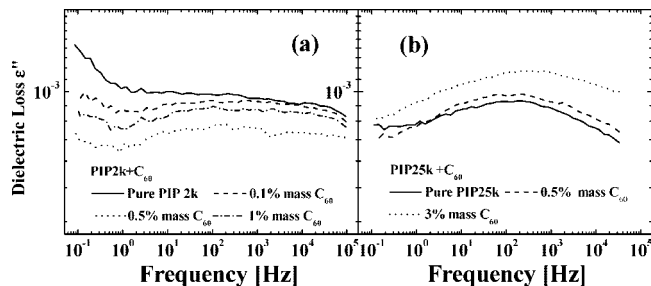


**Figure 2.** Representative dielectric loss spectra correspond to the secondary relaxation at  $-90\text{ }^{\circ}\text{C}$  of (a)  $\text{C}_{60}$ -PIP2k systems with different  $\text{C}_{60}$  concentration: solid line, neat PIP2k; dashed line, with 0.1% mass  $\text{C}_{60}$ ; dotted line, with 0.5% mass  $\text{C}_{60}$ ; dashed-dotted line, with 1% mass  $\text{C}_{60}$ . (b)  $\text{C}_{60}$ -PIP25k for different  $\text{C}_{60}$  concentrations: solid line, pure PIP25k; dashed line, with 0.5% mass  $\text{C}_{60}$ ; dotted line, with 3% mass  $\text{C}_{60}$ .

For the PIP2k nanocomposites with different  $\text{C}_{60}$  concentrations, the spectra show a broad excess wing-like secondary (or  $\beta$ ) relaxation with very small slope (near constant loss), consistent with previous literature reports.<sup>32–34,36–39,46–48</sup> However, a clear peak of the secondary relaxation appears in samples with higher molecular weight ( $\text{C}_{60}$ -PIP25k, Figure 2b). Such an enhanced  $\beta$  relaxation with an increase of molecular weight was also reported for polypropylene glycol, an effect probably associated with an enhanced fragility (temperature dependence of  $\alpha$ -relaxation time, shown below) due to the increase in chain length.<sup>49</sup> The amplitude of the relaxation process in polymers with both molecular weights is small (value of  $\epsilon'' \sim 10^{-3}$ ) and comparable to the instrumental limit of our spectrometer ( $\sim 10^{-4}$ ). Thus the observed variations in the amplitude of the  $\beta$  relaxation with the addition of fullerene (Figure 2) are unreliable. However, the frequency of the relaxation peak is reliable. A well resolved  $\beta$  relaxation peak in the  $\text{C}_{60}$ -PIP25k systems clearly moves to *higher frequency* with the addition of  $\text{C}_{60}$ . The  $\beta$ -peak is not so well resolved in PIP2k systems and we did not find a detectable change of the relaxation time with the  $\text{C}_{60}$  additive in this case.

For all our samples, we observe no qualitative changes in the shape of the relaxation modes with the  $\text{C}_{60}$  additive. In particular, the frequency dependence of  $\epsilon''(\omega)$  exhibits slope near  $-1$  in the low frequency regime (data not shown in figure) corresponding to the large scale “breathing” motion of the chains (normal mode relaxation). This trend is characteristic for the loss spectrum in the “terminal” relaxation regime governing large scale chain relaxation.<sup>28,29,50</sup>

The dielectric loss spectra were fitted by the Havriliak–Negami (HN) functions with additional conductivity contribution<sup>51</sup>

$$\epsilon^* = \epsilon_{\infty} + \sum_j \frac{(\Delta\epsilon)}{[1 + (i\omega\tau_j)^{\alpha}]^{\beta}} - \frac{i\sigma}{\epsilon_0\omega^s} \quad (1)$$

where  $\sigma$  is the conductivity,  $\omega$  is the angular frequency,  $s$  is the exponent describing conductivity slope,  $\tau_j$  is relaxation time of the  $j^{\text{th}}$  process,  $\epsilon_0$  is the vacuum permittivity,  $\Delta\epsilon$  is dielectric strength of the  $j^{\text{th}}$  process,  $\alpha$  and  $\beta$  are parameters that define symmetric and asymmetric broadening of the relaxation spectrum, respectively. A symmetric Cole–Cole function (corresponding to a shape parameter  $\beta = 1$  in the HN equation) was used for analysis of secondary relaxation spectra. Characteristic relaxation times for each processes were estimated as the reciprocal of the peak frequency  $\tau = 1/2\pi\omega_{\text{max}}$ .

Figure 3 shows the relaxation times for both the segmental and chain relaxation processes as a function of temperature for (a) PIP2k and (b) PIP25k with different  $\text{C}_{60}$  concentrations. Secondary relaxation times for the PIP25k system were also

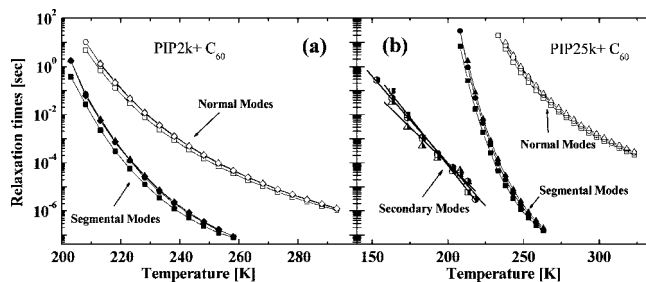


**Figure 3.** Relaxation times as a function of temperature for (a)  $\text{C}_{60}$ -PIP2k, and (b)  $\text{C}_{60}$ -PIP25k. For part a: squares, neat PIP2k; circles, 0.1 mass %  $\text{C}_{60}$ ; triangles, 0.5% mass  $\text{C}_{60}$ ; diamonds, 1% mass  $\text{C}_{60}$ . For part b: squares, neat PIP25k; circles, 0.5% mass  $\text{C}_{60}$ ; triangles, 3% mass  $\text{C}_{60}$ . The solid and empty symbols correspond to the segmental and chain relaxation modes, respectively. The half-filled symbols in part b represent the secondary relaxation times for corresponding concentrations.

presented in Figure 3b. Conventionally,  $T_g$  can be defined as the temperature at which the segmental relaxation time reaches 100 s. However, to avoid extrapolation of the data away from the accessible range of experimental time scales we used the arbitrary value 1 s for the estimation of  $T_g$  and the value obtained are listed in Table 1.<sup>52</sup> For both the unentangled and entangled PIP, there is an increase in  $T_g$  with the addition of  $\text{C}_{60}$ , in agreement with the measurement of  $\text{C}_{60}$ -PS by Sanz et al.<sup>16</sup> and Weng et al.<sup>24</sup> and  $\text{C}_{60}$ -PMMA systems by Kropka et al.<sup>20</sup> For PIP2k, the biggest change seems to occur between the pure and the lowest  $\text{C}_{60}$  concentration (0.1% mass) sample and no significant differences were observed for the other  $\text{C}_{60}$  concentrations. By comparison, a modest concentration dependence of  $T_g$  is found for the high molecular mass polymer nanocomposite. In contrast, the secondary relaxations time of PIP25k decreases with the addition of  $\text{C}_{60}$ , a trend *opposite* to that of the segmental and chain relaxation times. This result is consistent with the neutron measurements where an increase of Debye–Waller factor was observed, suggesting that the scale of the local chain motions are enhanced by the  $\text{C}_{60}$  additive so that the local “molecular stiffness” is decreased.<sup>16</sup>

From Figures 1 and 3, it is clear that both the segmental ( $\tau_{\alpha}$ ) and the chain ( $\tau_1$ ) relaxation times shift to a lower frequency with a decrease of temperature and these changes are well described by the Vogel–Fulcher–Tammann equation,<sup>29,30,53</sup>

$$\tau = \tau_0 \exp\left(\frac{DT_0}{T - T_0}\right) \quad (2)$$

where  $\tau_0$  is the relaxation time at infinite high temperature,  $T_0$  is the so-called Vogel temperature at which the relaxation time goes to infinity, and  $D$  is the parameter related to *fragility* of material.<sup>53</sup> A smaller value of  $D$  implies steeper temperature dependence of the relaxation time or a more “fragile” behavior. Table 1 lists the fitted parameters obtained from Figure 3.  $T_0$  increases modestly with the addition of  $\text{C}_{60}$ , similar to the trend for  $T_g$ . In comparison, the modest slowing down of both segmental and chain relaxation of our system is similar to the results reported for  $\text{C}_{60}$ -PMMA nanocomposites, where both an increase of  $T_g$  and the terminal (chain) relaxation time were observed.<sup>20</sup>

Figure 3 also indicates that the temperature dependence of  $\tau_{\alpha}$  is much stronger than  $\tau_1$  for all the samples especially at temperatures close to  $T_g$ , a behavior that we have emphasized in previous work.<sup>45</sup> Similarly, we plot the ratio of  $\tau_1$  to  $\tau_{\alpha}$  as a function of the temperature in Figure 4 for our  $\text{C}_{60}$ -PIP2k nanocomposites. For all other samples, this ratio shows a strong temperature dependence (Figure 4), consistent with ref 45. Since  $\tau_1$  and  $\tau_{\alpha}$  can only be simultaneously determined over a limited

**Table 1.**  $T_g$  and Parameters from the VFT Fit of Both the Segmental and Chain Relaxation Times

samples	$T_g \pm 1(\text{K})^a$ ( $\tau_\alpha = 1\text{s}$ )	segmental relaxation			chain relaxation			
		$\tau_0$ (s)	$D$	$T_0$ (K)	$\tau_0$ (s)	$D$	$T_0$ (K)	
PIP2k+ C <sub>60</sub>	0%	201.8	$1.5 \times 10^{-13}$	8.1	158.2	$1.2 \times 10^{-11}$	11.6	145.3
	0.1%	203.9	$1.3 \times 10^{-13}$	8.1	160.4	$1.4 \times 10^{-11}$	11.4	147.0
	0.5%	203.9	$8.7 \times 10^{-14}$	8.6	158.7	$1.4 \times 10^{-11}$	11.3	147.2
	1%	203.8	$3.2 \times 10^{-13}$	7.4	162.2	$2.0 \times 10^{-11}$	10.8	148.4
PIP25k+ C <sub>60</sub>	0%	210.9	$2.2 \times 10^{-13}$	7.5	168.0	$2.0 \times 10^{-8}$	9.5	159.9
	0.5%	212.9	$7.0 \times 10^{-13}$	8.4	166.9	$1.9 \times 10^{-8}$	9.7	160.1
	3%	214.0	$1.2 \times 10^{-13}$	7.9	169.1	$2.2 \times 10^{-8}$	9.5	161.1

<sup>a</sup> The error bars presented throughout this manuscript indicate the relative standard uncertainty of the measurement.

temperature range for the PIP25k series, we did not examine this ratio quantitatively for this sample.

We also see in Figure 4 that the ratio  $\tau_1/\tau_\alpha$  decreases with an increase of the C<sub>60</sub> concentration at a given temperature, i.e., the separation between the  $\tau_1$  and  $\tau_\alpha$  progressively decrease with the addition of C<sub>60</sub>. To illustrate this point, Figure 5 directly compares the dielectric spectra for the each PIP nanocomposites with different C<sub>60</sub> loading at representative temperature (218K for PIP2k system and 238K for PIP25k system). These spectra were normalized by a horizontal shift of the normal mode relaxation spectra of the low and high molecular mass polymers. No visible change in the spectral shape of chain relaxation modes is observed. In contrast, stronger variations of segmental relaxation modes are observed; there is in particular a marked increase of relaxation strength.

The relaxation strength of segmental and chain relaxation modes of polymers can be reasonably described by the Kirkwood–Frohlich relation,<sup>29,30</sup>

$$\Delta\epsilon_{\text{seg}} = g \frac{4\pi FN\rho}{3k_B T} \mu^2 \quad (3)$$

$$\Delta\epsilon_{\text{normal}} = g \frac{4\pi FN\rho}{3k_B T} \mu^2 \frac{\langle R^2 \rangle}{M} \quad (4)$$

where  $\rho$  is the density,  $F$  is the local field correction,  $\mu$  is the molecular dipole moment, and  $g$  is the Kirkwood–Frohlich correlation factor, which measures the correlation between dipole moments in neighboring units, and  $\langle R^2 \rangle$  refers to mean square of the end-to-end distance of the chain.

Since no variations in  $\Delta\epsilon_{\text{normal}}$  were observed, we do not expect significant change of  $\langle R^2 \rangle$  upon addition of C<sub>60</sub>. In addition, if chain or coil dilation due to the C<sub>60</sub> additives does occur, it should show a concentration dependence,  $R_{g,\text{composite}}/R_{g,\text{pure polymer}} = 1 + c\phi$ , where  $\phi$  is the concentration of the C<sub>60</sub> and  $c$  is a constant.<sup>21,54</sup> Such a dependence is absent from our measured spectra. This is clearly different from the observations that  $R_g$  of PS increase with the addition of PS-nanoparticles.<sup>54</sup> The discrepancies might be caused by different dispersion methods used for preparing the nanocomposites and the difference in the specific nanoparticle - polymer interactions determined by the chemical structures.

Compared with  $\Delta\epsilon_{\text{normal}}$ , we observed a progressive increase of  $\Delta\epsilon_{\text{segmental}}$  with C<sub>60</sub> concentrations for both PIP samples (Figure 5). We suggest that such an effect might be caused by the increase in  $g$ , i.e. with additions of C<sub>60</sub>, there is an increase in correlations of the neighboring dipole moments that contribute to segmental relaxations.<sup>55</sup> Apparently, such a perturbation is more localized to the type B dipole moment (perpendicular to the backbone, corresponds to the segmental relaxations), as no such change in the relaxation strength of the chain modes was observed.

Figure 6 compares the ratio between relaxation times for the C<sub>60</sub>–PIP composites and neat PIP as a function of temperature. In accord with the relaxation strength, the degree of retardation with addition of C<sub>60</sub> is much stronger for  $\tau_\alpha$  than  $\tau_1$ , and this

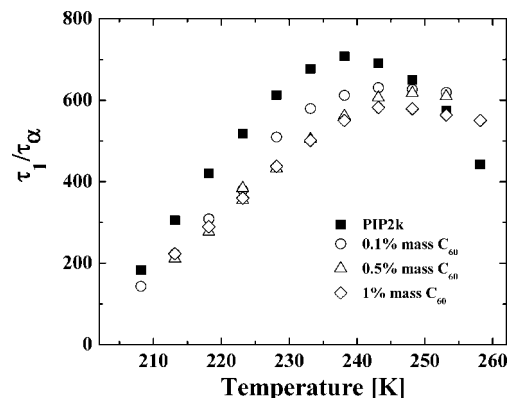


**Figure 4.** Ratio of chain to segmental relaxation times as a function of temperature for PIP2k with different C<sub>60</sub> concentrations: filled square, neat PIP2k; circle, 0.1% mass C<sub>60</sub>; triangle, 0.5% mass C<sub>60</sub>; diamond, 1% mass C<sub>60</sub>.

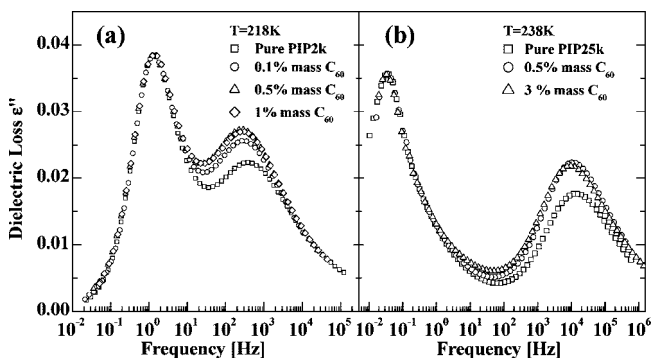


**Figure 5.** Dielectric relaxation spectra for (a) PIP2k with different C<sub>60</sub> concentrations at 218 K, and (b) PIP25k with different C<sub>60</sub> concentrations at 238 K. The spectra are shifted horizontally to match the chain relaxation (lower frequency) peak.

effect becomes more dramatic as temperature decreases. This result is very much in line with previous observations that factors (such as temperature and pressure) which strongly influence the segmental relaxation have a weakening effect on the chain relaxation process.<sup>34,45</sup> Although this phenomenon has not yet been given a general explanation, we can rationalize this trend based on the origin of the fragility of glasses in the entropy theory of glass formation developed by Dudowicz et al.<sup>56–58</sup>

According to this theory, when there is a significant degree of packing frustration, the fragility of glass formation should be higher and the transport properties are more sensitive to temperature or other perturbations that can influence the packing geometry. The segmental motions are dominated by strong local hard core repulsive interactions that limit the efficiency of local packing. At longer time scales (on the order of  $\tau_1$ ) and larger spatial scales (on the order of  $R_g$ ), the center of mass motion of the chains can be roughly described as interacting soft spheres because of their strong interpenetration.<sup>59–61</sup>

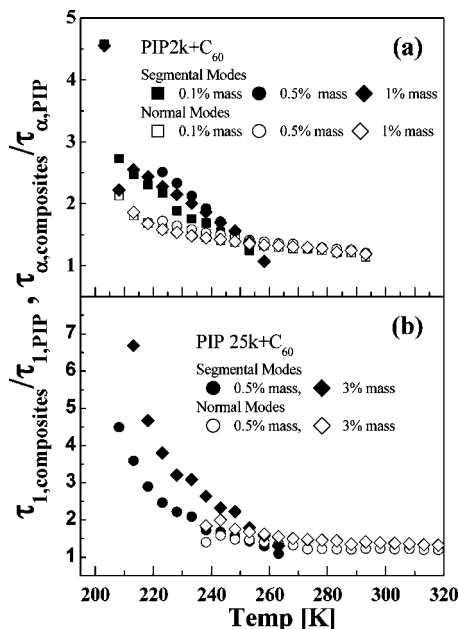


**Figure 6.** Ratio of segmental (filled symbols) and chain relaxation (empty symbols) of the PIP nanocomposites to that of the pure PIP: (a) PIP2k composites and (b) PIP25k composites.

From this perspective, the dynamics of flexible chains at the scale of  $R_g$  should be universally that of a strong glass-former (showing weak temperature dependence of  $\tau_1$ ) because of the relatively high packing efficiency of the soft spheres in comparison with hard spheres and other less penetrable particles. Moreover, the difference between the segmental and chain relaxation processes should be more prevalent in systems whose segmental relaxation process is characterized by a more fragile glass formation, associated with a high local packing frustration due to strong local excluded volume interactions.<sup>56–58</sup> Additives such as  $C_{60}$  that modify local molecular packing, and thus the local segmental relaxation process, should have a weaker effect on the scale of the polymer chains. In short, the heterogeneities prevalent at the segmental scales are not dominant at the scales of  $R_g$ .

This interpretation of the scale dependence of the fullerene additive on the dielectric relaxation is consistent with the trends observed in Figure 6, which indicate that the change of  $\tau_\alpha$  due to the addition of  $C_{60}$  becomes progressively larger than the change in  $\tau_1$  as the temperature approaches  $T_g$  and correspondingly the lifetime of the heterogeneity of the supercooled liquid at a nanoscale increases. Similarly, such a scale dependent perturbation of  $C_{60}$  on the PIP is consistent with the observation that the correlations between local dipoles (type B, segment scale) may be enhanced more than those between the chains (type A) (Figure 5).

Additives that disrupt molecular packing efficiency are also anticipated to increase fragility of glass formation, which physically should be signaled by a softening of the material in the glass state and a simultaneous increase in  $T_g$ . Our observations are consistent with a trend toward enhanced fragility induced by the  $C_{60}$  additive (although the effect is relatively small in PIP). A similar, but more substantial magnitude effect of this kind has been inferred from indirect neutron scattering measurements for  $C_{60}$ -PS nanocomposites.<sup>16</sup>

An enhanced fragility upon  $C_{60}$  addition should then lead to decrease in the  $\beta$  relaxation time, an effect opposite to the well documented “antiplasticization” phenomenon with molecular or nanoparticle additives. In a typical antiplasticization effect, the additives will cause an increase in the  $\beta$  relaxation time and decrease in both the  $\alpha$  relaxation time and fragility.<sup>62,63</sup> In our

$C_{60}$ -PIP25k samples, the observation of a decrease in the  $\beta$  relaxation time, with a simultaneous increase of the  $\alpha$  relaxation time, is consistent with an increase of fragility in PIP with the  $C_{60}$  additive (see Table 1). Unfortunately, the overall effect is rather weak, most likely due to the choice of a polymer (PIP) that is relatively strong to begin with. Recent molecular dynamics simulations by Starr and Douglas (unpublished work) show that nanoparticles with highly attractive interaction for the polymer matrix can render the nanocomposite more fragile, similar to our  $C_{60}$ -PIP system, and the neutron measurements of  $C_{60}$ -PS system.

The  $\beta$  relaxation time is also phenomenologically linked to the mechanical properties of polymer materials (shear modulus, brittleness, toughness, impact strength)<sup>62,63</sup> and a better understanding of how nanoparticles can modulate this basic fluid property has obvious practical, as well as scientific interest. We plan to use dielectric spectroscopy to investigate the variation of the  $\beta$  relaxation time for other nanoparticle-polymer pairs in the future and the implications of these changes for other polymer properties.

Finally, we remark on the general problem of nanoparticle clustering and the possible effect of this phenomenon on our observations. As noted earlier, previous work has established a general tendency toward large-scale  $C_{60}$  clustering starting from concentrations  $\varphi = 2\%$  mass to  $\varphi = 3\%$  mass and nanoscale clustering develops for concentrations around 1% mass. Our study covers this concentration range, but also includes data for low concentration regime ( $\varphi = 0.5\%$  mass), where appreciable clustering should be absent. Since the effects we observe are apparent at this low concentration, it is difficult to attribute the opposite trends in the shift in  $\beta$  and segmental (also terminal relaxation) times to large-scale particle clustering.

## Conclusions

Dielectric spectroscopy was used to investigate the influence of  $C_{60}$  nanoparticle additives on the secondary, segmental and chain relaxation processes for both unentangled and entangled PIP. Both segmental and chain relaxation processes become slower with the  $C_{60}$  addition, an effect associated with an increase of the glass transition temperature and/or an enhanced molecular friction coefficient. However, the extent of this retardation effect is strongly *scale dependent*. Detailed comparisons show that the segmental relaxation exhibits a stronger sensitivity to the  $C_{60}$  additives than the chain relaxation, and this effect become increasingly dramatic with decrease of temperature. We attribute this effect to the varying extent of packing frustrations on the chain and segmental length scales.

In contrast to the segmental and chain relaxation processes, the secondary or  $\beta$  relaxation process of entangled PIP was observed to *speed up* with addition of  $C_{60}$ . This observation agrees with the recent neutron measurements where local softening of PS upon  $C_{60}$  additions was observed, while the  $T_g$  was reported to increase. These observations suggest that nanoparticles can have a *qualitatively* different effect on the matrix polymer dynamics at different length scales, and thus caution must be taken in comparing changes in the dynamics associated with different relaxation processes.

**Acknowledgment.** S.P. acknowledges the financial assistance from FNP HOMING program (2008) supported by the European Economic Area Financial Mechanism. A.P.S. thanks the NSF for financial support. Y.D. acknowledges the startup funding support from University of Colorado at Boulder. Certain commercial materials and equipment are identified in this paper in order to specify adequately the experimental procedure. In no case does such identification imply recommendation by the National Institute of

Standards and Technology nor does it imply that the material or equipment identified is necessarily the best available for this purpose.

## References and Notes

- (1) Wang, D. Z.; Zuo, J.; Zhang, Q. J.; Luo, Y.; Ruan, Y. Z.; Wang, Z. *J. Appl. Phys.* **1997**, *81*, 1413.
- (2) Higuchi, A.; Agatsuma, T.; Uemiya, S.; Kojima, T.; Mizoguchi, K.; Pinnau, I.; Nagai, K.; Freeman, B. D. *J. Appl. Polym. Sci.* **2000**, *77*, 529.
- (3) Holmes, M. A.; Mackay, M. E.; Giunta, R. K. *J. Nanoparticle Res.* **2007**, *9*, 753.
- (4) Hoppe, H.; Sariciftci, N. S. *J. Mater. Res.* **2004**, *19*, 1924.
- (5) Rapoport, L.; Fleischer, N.; Tenne, R. *Adv. Mater.* **2003**, *15*, 651.
- (6) Yu, G.; Gao, J.; Hummelen, J. C.; Wudl, F.; Heeger, A. J. *Science* **1995**, *270*, 1789.
- (7) Mackay, M. E.; Tuteja, A.; Duxbury, P. M.; Hawker, C. J.; Van Horn, B.; Guan, Z. B.; Chen, G. H.; Krishnan, R. S. *Science* **2006**, *311*, 1740.
- (8) Krishnamoorti, R.; Vaia, R. A. *J. Polym. Sci., Part B: Polym. Phys.* **2007**, *45*, 3252.
- (9) Barnes, K. A.; Karim, A.; Douglas, J. F.; Nakatani, A. I.; Gruell, H.; Amis, E. J. *Macromolecules* **2000**, *33*, 4177.
- (10) Fang, Z. P.; Song, P. A.; Tong, L. F.; Guo, Z. H. *Thermochim. Acta* **2008**, *473*, 106.
- (11) Song, P.; Zhu, Y.; Tong, L. F.; Fang, Z. P. *Nanotechnology* **2008**, *19*, 255707.
- (12) Tsuji, H.; Kawashima, Y.; Takikawa, H. *J. Polym. Sci., Part B: Polym. Phys.* **2007**, *45*, 2167.
- (13) Paul, S.; Kanwal, A.; Chhowalla, M. *Nanotechnology* **2006**, *17*, 145.
- (14) Antipov, O. L.; Yurasova, I. V.; Domrachev, G. A. *Quant. Electron.* **2002**, *32*, 776.
- (15) Kropka, J. M.; Sakai, V. G.; Green, P. F. *Nano Lett.* **2008**, *8*, 1061.
- (16) Sanz, A.; Ruppel, M.; Douglas, J. F.; Cabral, J. T. *J. Phys.: Condens. Matter* **2008**, *20*, 104209.
- (17) Papakonstantopoulos, G. J.; Yoshimoto, K.; Doxastakis, M.; Nealey, P. F.; de Pablo, J. J. *Phys. Rev. E* **2005**, *72*, 031801.
- (18) Riggelman, R. A.; Douglas, J. F.; de Pablo, J. J. *J. Chem. Phys.* **2007**, *126*, 234903.
- (19) Arceo, A.; Meli, L.; Green, P. F. *Nano Lett.* **2008**, *8*, 2271.
- (20) Kropka, J. M.; Putz, K. W.; Pryamitsyn, V.; Ganesan, V.; Green, P. F. *Macromolecules* **2007**, *40*, 5424.
- (21) Tuteja, A.; Duxbury, P. M.; Mackay, M. E. *Macromolecules* **2007**, *40*, 9427.
- (22) Tuteja, A.; Mackay, M. E.; Narayanan, S.; Asokan, S.; Wong, M. S. *Nano Lett.* **2007**, *7*, 1276.
- (23) Mijovic, J.; Lee, H. K.; Kenny, J.; Mays, J. *Macromolecules* **2006**, *39*, 2172.
- (24) Weng, D.; Lee, H. K.; Levon, K.; Mao, J.; Scrivens, W. A.; Stephens, E. B.; Tour, J. M. *Eur. Polym. J.* **1999**, *35*, 867.
- (25) Knauert, S. T.; Douglas, J. F.; Starr, F. W. *J. Polym. Sci., Part B: Polym. Phys.* **2007**, *45*, 1882.
- (26) Bansal, A.; Yang, H. C.; Li, C. Z.; Cho, K. W.; Benicewicz, B. C.; Kumar, S. K.; Schadler, L. S. *Nat. Mater.* **2005**, *4*, 693.
- (27) Wang, X. R.; Yan, Y. Y. *Polymer* **2006**, *47*, 6267.
- (28) Adachi, K.; Kotaka, T. *Prog. Polym. Sci.* **1993**, *18*, 585.
- (29) Watanabe, H. *Macromol. Rapid Commun.* **2001**, *22*, 127.
- (30) Kremer, F.; Schönhals, A. *Broadband Dielectric Spectroscopy*; Springer: New York, 2003.
- (31) Stockmayer, W. H. *Pure Appl. Chem.* **1967**, *15*, 539.
- (32) Roland, C. M.; Ngai, K. L. *Macromolecules* **1991**, *24*, 5315.
- (33) Boese, D.; Kremer, F. *Macromolecules* **1990**, *23*, 829.
- (34) Floudas, G.; Reisinger, T. *J. Chem. Phys.* **1999**, *111*, 5201.
- (35) Lee, H. K.; Pejanovic, S.; Mondragon, I.; Mijovic, J. *Polymer* **2007**, *48*, 7345.
- (36) Adachi, K.; Kotaka, T. *Macromolecules* **1984**, *17*, 120.
- (37) Schonhals, A. *Macromolecules* **1993**, *26*, 1309.
- (38) Watanabe, H.; Urakawa, O.; Yamada, H.; Yao, M. L. *Macromolecules* **1996**, *29*, 755.
- (39) Santangelo, P. G.; Roland, C. M. *Macromolecules* **1998**, *31*, 3715.
- (40) Fetters, L. J.; Lohse, D. J.; Richter, D.; Witten, T. A.; Zirkel, A. *Macromolecules* **1994**, *27*, 4639.
- (41) Zhang, C.; Xiao, X. D.; Ge, W. K.; Loy, M. M. T.; Wang, D. Z.; Zhang, Q. J.; Jian, Z. *Appl. Phys. Lett.* **1996**, *68*, 943.
- (42) Peng, H.; Leung, F. S. M.; Wu, A. X.; Dong, Y. P.; Dong, Y. Q.; Yu, N. T.; Feng, X. D.; Tang, B. Z. *Chem. Mater.* **2004**, *16*, 4790.
- (43) Zolotukhin, I. V.; Yanchenko, L. I.; Belonogov, E. K. *JETP Lett.* **1998**, *67*, 720.
- (44) Han, J.; Lee, G.; Kim, S.; Lee, H.; Douglas, J. F.; Karim, A. *Nanotechnology*, in press.
- (45) Ding, Y. F.; Sokolov, A. P. *Macromolecules* **2006**, *39*, 3322.
- (46) Dalal, E. N.; Phillips, P. J. *Macromolecules* **1983**, *16*, 890.
- (47) Doxastakis, M.; Theodorou, D. N.; Fytas, G.; Kremer, F.; Faller, R.; Muller-Plathe, F.; Hadjichristidis, N. *J. Chem. Phys.* **2003**, *119*, 6883.
- (48) Arbe, A.; Colmenero, J.; Alvarez, F.; Monkenbusch, M.; Richter, D.; Farago, B.; Frick, B. *Phys. Rev. E* **2003**, *67*, 051802.
- (49) Mattsson, J.; Bergman, R.; Jacobsson, P.; Borjesson, L. *Phys. Rev. Lett.* **2003**, *90*, 075702.
- (50) Ferry, J. D. *Viscoelastic Properties of Polymers* 3rd ed.; John Wiley & Sons: New York, 1980.
- (51) Havriliak, S.; Negami, S. *J. Polym. Sci., Part C: Polym. Symp.* **1966**, *99*.
- (52) Paluch, M.; Pawlus, S.; Roland, C. M. *Macromolecules* **2002**, *35*, 7338.
- (53) Angell, C. A.; Ngai, K. L.; McKenna, G. B.; McMillan, P. F.; Martin, S. W. *J. Appl. Phys.* **2000**, *88*, 3113.
- (54) Tuteja, A.; Duxbury, P. M.; Mackay, M. E. *Phys. Rev. Lett.* **2008**, *100*, 077801.
- (55) Casalini, R.; Roland, C. M. *Macromolecules* **2005**, *38*, 1779.
- (56) Dudowicz, J.; Freed, K. F.; Douglas, J. F. *J. Phys. Chem. B* **2005**, *109*, 21350.
- (57) Dudowicz, J.; Freed, K. F.; Douglas, J. F. *J. Chem. Phys.* **2006**, *124*, 14.
- (58) Dudowicz, J.; Freed, K. F.; Douglas, J. F. *Generalized Entropy Theory of Polymer Glass Formation*; Wiley: New York, 2008; Vol. 137.
- (59) Guenza, M. G. *J. Phys.: Condens. Matter* **2008**, *20*, 033101.
- (60) Yatsenko, G.; Sambriski, E. J.; Guenza, M. G. *J. Chem. Phys.* **2005**, *122*, 054907.
- (61) Yatsenko, G.; Sambriski, E. J.; Nemirovskaya, M. A.; Guenza, M. *Phys. Rev. Lett.* **2004**, *93*, 257803.
- (62) Psurek, T.; Soles, C. L.; Page, K. A.; Cicerone, M. T.; Douglas, J. F. *J. Phys. Chem. B* **2008**, *112*, 15980.
- (63) Anopchenko, A.; Psurek, T.; VanderHart, D.; Douglas, J. F.; Obrzut, J. *Phys. Rev. E* **2006**, *74*, 031501.

MA8024333